SPH Modelling of a 3D Tsunami Test Case

Roberto Guandalini[1], Giordano Agate[1], Andrea Amicarelli[1*], Sauro Manenti[2], Mario Gallati[2], Stefano Sibilla[2]

[1]Ricerca sul Sistema Energetico RSE SpA, Department SFE (Sustainable Development and Energy Sources, formerly ASV), via Rubattino 54, 20134, Milan, Italy
[2] Dept. of Civil Engineering and Archtecture, University of Pavia, Pavia, Italy

roberto.guandalini@rse-web.it; giordano.agate@rse-web.it; andrea.amicarelli@rse-web.it; sauro.manenti@unipv.it; gallati@unipv.it; stefano.sibilla@unipv.it

Abstract

Tsunami-induced coastal floods are relevantly represented among the deadliest and costliest disasters ever. In this context, several numerical techniques have been studied for prevention, protection and planning activities, for both catastrophic and more frequent events. An effective solution is provided by the SPH method, a mesh-less CFD (Computational Fluid Dynamics) technique, particularly suitable for flood event modelling.

This study describes the validation of a 3D "Weakly-Compressible" SPH (Smoothed Particle Hydrodynamics) model, considering a 3D tsunami test case (Benchmark 1-2009 of ISEC-Inundation Science&Engineering Cooperative-).

The model satisfactorily reproduces the sea level and velocity time series, recorded at the monitoring points. The results show the reliability and the further potentials of the model in representing a 3D generation and propagation of a solitary wave with the consequent coastal flood.

Finally this study seems to represent one of the first validations of a 3D SPH model on a tsunami test case.

Keywords

SPH; Tsunami; Surface Waves; Floods; Wave Motion; Solitary Wave

Introduction

Flood events have caused huge damages to human health, environment, anthropic structures and infrastructures. In particular, tsunami-induced coastal floods are heavily represented in both deadliest flood events and costliest disasters ever.

The five deadliest floods, causing over $2.0*10^5$ casualties, are cited in the following. After some years of drought, the Central China floods of 1931 (due to several months of huge precipitations) caused more than $2.5*10^6$ dead. Yellow River (China) was interested by two huge floods, responsible for more than $9.0*10^5$ casualties in 1887 and more than $5*10^5$ dead in 1938. Around $2.3*10^5$ individuals died because of a dam break event (Banqiao, typhoon Nina, China 1975). Finally, an Indian Ocean tsunami caused around $2.3*10^5$ casualties in Indonesia (2004).

On the other hand, the costliest floods ever are represented by the following events (damage over 5 billions USA dollars -USD- each):

- $300*10^9$USD: Tōhoku earthquake and tsunami (2011, Japan), the costliest disaster ever, the most damage were due to the tsunami coastal flood;
- $46*10^9$USD: Thailand riverine and areal floods due to monsoons (2011);
- $26*10^9$USD. 1998 Yellow river floods;
- $7.0*10^9$USD. Armero tragedy (Colombia, 1985, pyroclastic flow floods);
- $5.0*10^9$USD: 2013 Alberta (riverine and areal) floods (Canada).

In this frame, several numerical techniques have been studied in order to simulate flood events (e.g. Le Veque et al. 2007), for prevention, protection and planning activities. Among the others, SPH (Smoothed Particle Hydrodynamics) method is particularly suitable for modelling these phenomena, such as coastal floods (caused by solitary waves/tsunamis, etc.), dam breaks (e.g. Grenier et al. 2009, Di Monaco et al. 2011, Amicarelli et al. 2013), riverine and areal floods, urban flooding, tank leakages (e.g. Maurel et al. 2009), floods caused by landslides or volcanic activities, etc.

SPH is a mesh-less Computational Fluid Dynamics (CFD) technique, whose computational nodes are represented by numerical fluid particles. In the continuum, the functions and derivatives appearing in the governing balance equations of fluid mechanics are approximated using convolution integrals over smoothing functions. Then for a generic function f the SPH integral approximation (<>I) is provided by:

$$\langle f \rangle_{I,\underline{x}_0} = \int_{V_h} f W dx^3 \qquad (1)$$

where W is a weighting function (called kernel), $\underline{x}_0$ is the position of a generic computational point and V_h the integration volume called kernel support (a sphere of radius 2h in the inner domain, far from boundaries), whose characteristic length is h. A generic first order derivative along x_i direction can be still computed as in (1). After integration by parts, it takes the form:

$$\left\langle \frac{\partial f}{\partial x_i} \right\rangle_{I,\underline{x}_0} = \int_{A_h} f W n_i dx^2 - \int_{V_h} f \frac{\partial W}{\partial x_i} dx^3 \qquad (2)$$

Here a surface integration is considered all over the surface (A_h) of the kernel support. This term is peculiar and necessary at boundaries, where the kernel support is truncated by the fluid domain frontiers and SPH truncation errors noticeably grow (Amicarelli et al., 2011a and 2011b). The modelling of this term can relevantly differentiate SPH models and is still object of recent studies (Adami et al. 2012, Hashemi et al. 2012, Macia et al. 2012, Mayrhofer et al. 2013, Ferrand et al. 2013, Amicarelli et al. 2013,).

SPH technique has several advantages:

- direct estimation of free surface and phase/ fluid interfaces;
- effective simulation of multiple moving bodies and particulate matter within fluid flows;
- direct estimation of Lagrangian derivatives (absence of non-linear convective terms in the balance equation Left-Hand Sides);
- effective numerical simulations of fast transient phenomena;
- no meshing;
- simple and non-iterative algorithm.

On the other hand, SPH models are still affected by a few shortcomings, if compared with mesh-based CFD tools:

- higher computational time consumption at the same resolution (mean feature);
- limited accuracy, if considered as a general purpose CFD technique.

SPH models are effective in several, but peculiar, application fields. Some of them are here briefly recalled: floods; sloshing (e.g. oscillatory flows within tanks, Souto-Iglesias et al. 2006, Delorme et al. 2009, Amicarelli et al. 2013); gravitational surface waves (e.g. Manenti et al. 2008, Patel et al. 2009, Antuono et al. 2011, Liu et al. 2013, Omidvar et al. 2013, Farahani et al. 2014); hydraulic turbines (Marongiu et al. 2009, Neuhauser et al. 2013); fast landslides (Kumar et al. 2013); hydroelectric plant devices; bed load transport and erosion phenomena (Manenti et al., 2009 and 2012, Manenti 2011, Guandalini-Agate, 2011); liquid jets (Koukouvinis et al. 2013); pollutant dispersion; astrophysics (e.g. Price and Monaghan 2007; Bauer and Spingel 2012); magnetohydrodynamics (e.g. Price 2012); multi-phase and multi-fluid flows (e.g. Kajtar-Monaghan, 2012). 2D SPH tsunami modelling (Shallow Water approximation) has been already tested, considering the ISEC 2004 Benchmark2, which reproduces Okushiri tsunami (Vacondio et al. 2012).

However, it seems there is a general lack of numerical model validations on complex tsunami events and coastal floods, especially in 3D.

In this context, this study is focused on the validation of the recent SPH model (Di Monaco et al., 2011) on a reference 3D tsunami test case (Benchmark 1-2009, ISEC). After this introduction, we recall the main features of the numerical model (Sec.2). We then describe the reference tsunami test case and the numerical configuration (Sec.3). Further we show and discuss the results (Sec.4) and we finally report the overall conclusions (Sec.5).

The SPH Numerical Model

The numerical model used for this validation is based on the semi-analytic approach for complex boundary treatment (Vila, 1999). Its basic features are deeply described in Di Monaco et al. (2011) and here briefly reported.

Navier-Stokes equation and the continuity equation are first considered in the continuum:

$$\frac{du_i}{dt} = -\frac{\partial\left(p/\rho\right)}{\partial x_i} - \frac{p}{\rho^2}\frac{\partial \rho}{\partial x_i} - \delta_{i3} g + \upsilon \frac{\partial^2 u_i}{\partial x_j^2}, i = 1,2,3 \qquad (3)$$

$$\frac{d\rho}{dt} = -\rho div\underline{u}$$

where u is the velocity vector, p pressure, ρ the fluid density, δ_{ij} Kronecker's delta and t time (Einstein notation works for "j"). The pressure gradient term has been split after a simple product rule for derivatives, in order to be more easily treated. In fact these equations are then elaborated using the SPH particle approximation of (2) and computed at each fluid particle position, as described in the following. The viscosity term for compressible fluids can be neglected in Navier Stokes equation, even if we adopt a Weakly Compressible fluid approach.

The SPH particle (discrete) approximation of a generic

derivative (2) can be computed at boundaries, according to the semi-analytic approach ("SA"):

$$\left\langle \frac{\partial f}{\partial x_i} \right\rangle_{SA} = \sum_b \left(f_b - f_0 \right) \frac{\partial W_b}{\partial x_i} \omega_b + \int_{V_h'} \left(f - f_0 \right) \frac{\partial W_b}{\partial x_i} dx^3 \quad (4)$$

The summation is performed over all the fluid particles "b" (neighbouring particles of volume ω) lying in the kernel support of the computational fluid particle ("0"). This formula also shows a boundary term, which is a convolution integral on the portion of the kernel support, lying outside the fluid domain. This portion then completes the kernel support, when it is truncated by boundaries. In this outer and fictitious volume (V_h'), we need to define a generic function f (pressure, velocity or density alternatively) to provide the proper boundary conditions. The semi-analytic approach, as developed by Di Monaco et al. (2011), follows this hypothesis:

$$\begin{aligned} & f \cong f_{SA} + \left. \frac{\partial f}{\partial x_i} \right|_{SA} \left(\underline{x} - \underline{x}_0 \right) \Rightarrow \\ & \Rightarrow \left\langle \frac{\partial f}{\partial x_i} \right\rangle_{SA} = \sum_b \left(f_b - f_0 \right) \frac{\partial W_b}{\partial x_i} \omega_b + \\ & + \int_{V_h'} f_{SA} \frac{\partial W_b}{\partial x_i} dx^3 + \int_{V_h'} \left. \frac{\partial f}{\partial x_i} \right|_{SA} \left(\underline{x} - \underline{x}_0 \right) \frac{\partial W_b}{\partial x_i} dx^3 \end{aligned} \quad (5)$$

The functions and derivatives of these first order Taylor approximations are then assigned according to the following assumptions:

$$\begin{aligned} & p_{SA} = p_0, \qquad \left\langle \frac{\partial p}{\partial x_i} \right\rangle_{SA} = -\delta_{i3} g; \\ & \rho_{SA} = \rho_0, \qquad \left\langle \frac{\partial \rho}{\partial x_i} \right\rangle_{SA} = 0 \end{aligned} \quad (6)$$

These conditions try to represent a null normal gradient for the pressure displacement from hydrostatic conditions. Density is approximately considered to be a constant within the outer support V_h' (of the ongoing computational particle).

At the same time, free-slip conditions can be approximately set when estimating velocity in V_h'. The velocity vector is assumed uniform in this region (still depending on the computational particle). It is decomposed in the sum of a vector normal to the boundary $\left(\underline{u}_{SA,n} \right)$ and the one tangential to it $\left(\underline{u}_{SA,T} \right)$. The first is represented by a linear extrapolation of the corresponding component of the computational fluid particle velocity. The latter is equal to the analogous value of the same particle (the subscript "w" refers to the local truncating frontier):

$$\underline{u}_{SA} = \underline{u}_{SA,T} + \underline{u}_{SA,n} \equiv \left(1 - \varphi_s \right) u_{0,T} + \left[\left(2\underline{u}_w - \underline{u}_0 \right) \cdot \underline{n}_w \right] \underline{n}_w \quad (7)$$

In this case ϕ_s is zero (free-slip conditions; for no-slip conditions ϕ_s=1).

The continuity equation ("Weakly-Compressible" SPH approach) can then be derived (Einstein's notation works for "j"):

$$\begin{aligned} & \frac{d\rho_0}{dt} = \sum_b \rho_b \left(u_{b,j} - u_{0,j} \right) \left. \frac{\partial W}{\partial x_j} \right|_b \omega_b + \\ & + 2\rho_0 \int_{V_h'} \left[\left(\underline{u}_w - \underline{u}_0 \right) \cdot \underline{n} \right] n_j \frac{\partial W}{\partial x_j} dx^3 \end{aligned} \quad (8)$$

Finally the approximation of the momentum equation provides the following expression:

$$\begin{aligned} & \left\langle \frac{du_i}{dt} \right\rangle_0 = -\delta_{i3} g + \\ & + \sum_b \left(\frac{p_b}{\rho_b^2} + \frac{p_0}{\rho_0^2} \right) \left. \frac{\partial W}{\partial x_i} \right|_b \frac{m_b}{\rho_b} + 2 \frac{p_0}{\rho_0} \int_{V_h'} \frac{\partial W}{\partial x_i} dx^3 + \\ & + 2\upsilon \sum_b \frac{m_b}{\rho_0 r_{0b}} \left(\underline{u}_b - \underline{u}_0 \right) \left. \frac{\partial W}{\partial r} \right|_b + \\ & + 2\varphi_s \upsilon \left(u_{w,i} - u_{0,i} \right) \cdot \left(\int_{V_h'} \frac{1}{r_{0w}} \frac{\partial W}{\partial r} dx^3 \right) + \\ & - \upsilon_M \sum_b \frac{m_b}{\rho_0 r_{0b}^2} \left(\underline{u}_b - \underline{u}_0 \right) \cdot \left(\underline{x}_b - \underline{x}_0 \right) \left. \frac{\partial W}{\partial x_i} \right|_b + \\ & - \upsilon_M \left(\underline{u}_{SA} - \underline{u}_0 \right) \cdot \left(\int_{V_h'} \frac{1}{r_{0w}^2} \left(\underline{x} - \underline{x}_0 \right) \frac{\partial W}{\partial x_i} dx^3 \right) \end{aligned} \quad (9)$$

ν_M represents the artificial viscosity (Monaghan, 2005), m the particle mass and r the relative distance between the neighbouring particle/boundary and the computational particle.

The second and third terms in the Right-Hand Side of (9) represent the inner and boundary terms related to pressure gradients. The next summation (Basa et al. 2009) and integral represent the molecular viscous terms (the latter being proposed only for no-slip conditions by Di Monaco et al. 2011, but not yet validated in 3D). We finally have two artificial viscosity terms, commonly used to stabilize SPH models and defined by Monaghan (2005, inner term) and Di Monaco et al. 2011 (boundary term). They are here activated, only for computational particles approaching neighbouring particles or boundaries, according to Di Monaco et al. (2011).

Time integration is performed with a staggered first order Euler scheme, where the continuity equation is translated in time of dt/2 with respect to the momentum equation (Di Monaco et al. 2011, Violeau-Leroy 2014).

Finally a barotropic equation of state is linearized for small density oscillations as follows (c_{ref} and ρ_{ref} are the

reference sound speed and density):

$$p \cong c_{ref}^2 \left(\rho - \rho_{ref} \right) \quad (10)$$

The 3D Tsunami Test Case

The reference benchmark was proposed by the Johns Hopkins University and belongs to ISEC database. The 3D domain and monitoring points are shown in FIG 1.

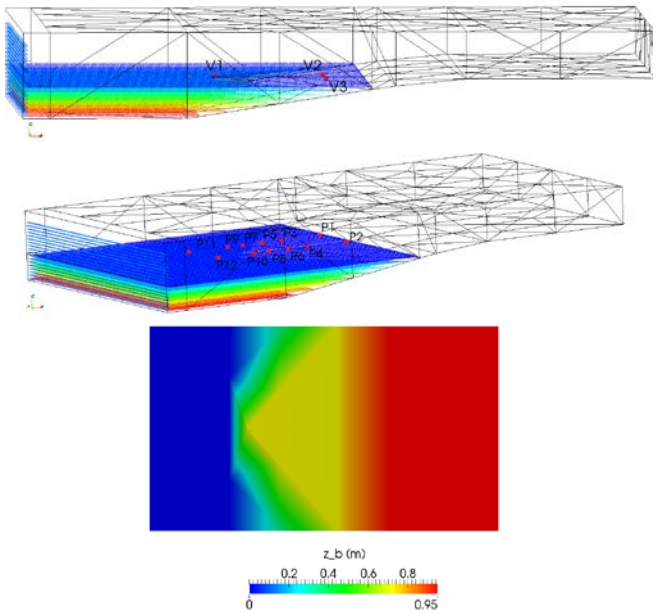

FIG. 1 TOP: 3D DOMAIN, WAVEMAKER AND VELOCITY MONITORING POINTS (V1-3). CENTRE: SEA LEVEL MONITORING LINES (P1-12). BOTTOM: HEIGHT OF THE FLUID-BOTTOM INTERFACE (batimetry). THE PADDLE (wavemaker) IS SIMULATED USING SPH PARTICLES WITH IMPOSED PARAMETERS. THE VERTICAL AXIS IS STRETCHED BY A FACTOR OF 2, IN ALL THE FIGURES.

A solitary wave (or tsunami) is generated on the left of the domain and propagates over a pyramidal shaped inclined shelf. In particular, a wave generator (left-side of the domain) produces a wave of amplitude h*=0.39 m over the quiet free surface elevation (z=0.78 m; the origin of the vertical axis is provided by the lowest point in the domain). The tsunami propagates towards the coastline (right-side of the domain). The irregular shelf is represented by a flat bottom, which evolves into an inclined shelf close to the the coast, at whose centre a pyramidal structure rises up. The overall phenomenon lasts 45s, but the most dynamics refers to the first 15-20s.

The numerical simulation has been configured accordingly to the experimental intial and boundary conditions. The parallelepiped inscribing the numerical domain is approximately 70x45x3 m^3 sized. The ratio between the kernel length size (h) and the particle size (dx) is equal to h/dx=1.25, with approximately dx=0.100 m. Time integration is performed choosing a high CFL (Courant-Friedrichs-Lewy) number of around 0.7, using a staggered Euler scheme. The wave generator movement is imposed, according to the experimental dataset. The lateral boundaries are fixed (semi-analytical approach) and water can move beyond the coast-line.

Results

The model results are here presented in terms of pressure and velocity fields, together with validations of the numerical sea level and velocity time series.

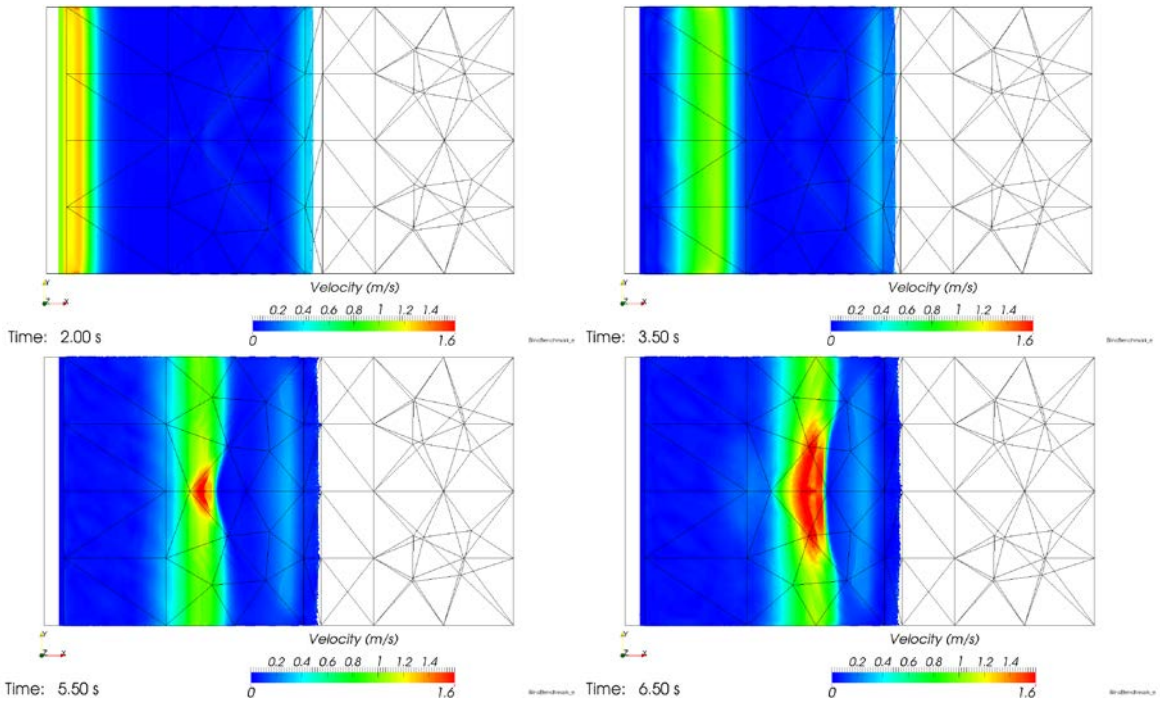

FIG. 2 3D FIELDS OF THE ABSOLUTE VALUE OF VELOCITY (top views).

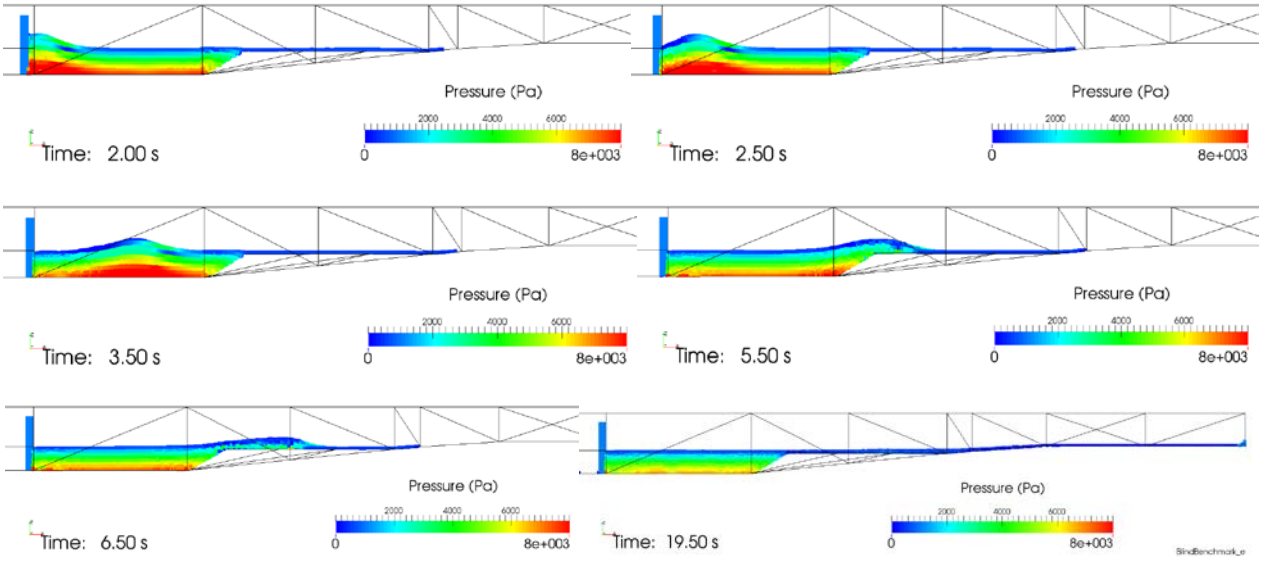

FIG. 3 SEQUENCE OF PRESSURE 3D FIELDS (vertical slice through the symmetry plane of the promontory).

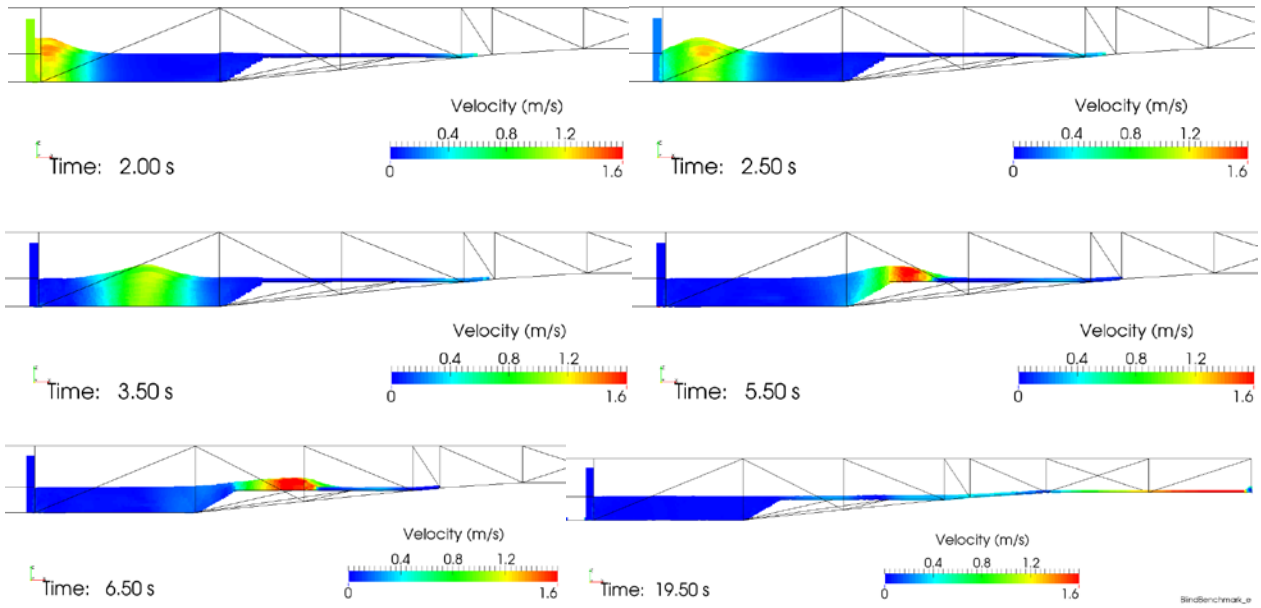

FIG. 4 SEQUENCE OF 3D FIELDS OF THE ABSOLUTE VALUE OF VELOCITY (vertical slice through the symmetry plane of the promontory).

FIG 2 reports a sequence of velocity fields (top views). The wave generation lasts around 3s. The first stage of the wave propagation is mainly 2D (t=3.5s). When the tsunami reaches the submerged promontory (t=5.5s), the wave group speed has a local minimum (lowest bottom depth). It gradually increases towards the lateral boundaries of the domain, with an increasing bottom depth (at the same time the surface fluid velocity is highest over the promontory and decreseas far away). The wave direction locally converges to the promontory axis (wave refraction) while the wave begins to break (t around 6.5s). The phenomenon is affected by wave reflections both at the left and right domain boundaries. Wave interactions, minor stationary structures and jumps locally take place, until water reaches again an almost quiet equilibrium (after t=30-35s).

The 3D fields of pressure and velocity are also described by a sequence of vertical slices passing for the promontory barycentres (FIG 3 and FIG 4).

Pressure can locally fluctuate around the local hydrostatic vertical profiles (FIG 3). Despite some small-scale anomalies and a very few fluid particles penetrating the wavemaker, the model represents a regular pressure field and the limited errors do not propagate in time. Moreover we are not interested in very accurate estimations of pressure forces at boundaries, as this study focuses on the assessment of sea levels and velocity during a tsunami event.

The sequence of fields in FIG 4 shows the time and space distribution of velocity, whose maximum values reach around 1.6-1.8m/s. Velocity decreases from the free surface to the bottom, or moving far away from the solitary wave crests. High velocities are simulated in the breaking zone, then close to the paddle (during the wave generation) and beyond the coastline, during the flood. This event can be clearly detected at t=19.5s, with water covering more than a tenth of meters beyond the original coastline. Some details of the wave breaking are clearly represented in FIG. 5, which refers to a further simulation, with a slightly higher resolution (dx=0.08m) than the reference simulation.

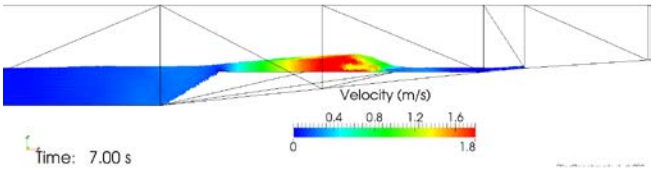

FIG. 5 Details of the wave breaking (dx=0.08m).

Validations are performed against measures from 15 monitoring points or lines. All the plots are normalized using reference height (h*=0.390m), velocity $\left(u^* = \sqrt{2gh^*} = 2.76m\right)$ and time scale t*(=h*/u* =0.141s), so that we treat non-dimensional variables (H=h/h*, U=u/u*, T=t/t*).

In particular, velocity estimations are validated in terms of time series of the x-component (u) of the mean velocity, at three monitoring points (V1-3).

The monitor V1 is placed along the vertical line crossing the vertex of the promontory (FIG 1). Its position, expressed in meters, is (13.00; 0.00; 0.75 m). The main forward and backward movements of water occur between T=32 and T=70. In this period we register the passage of the solitary wave, with water particles describing elliptical-like non-stationary trajectories. After this period a secondary wave is detected. The simulated values correctly reproduce the main features of u time evolution, even if some underestimations affect the amplitude of the peaks.

The velocity monitors V2 and V3 (FIG 1, centre and bottom, respectively) are closer to the coastline than V1 and transversally displaced with respect to the promontory. In these cases the measured time series show some lack of data (reference: ISEC web site). However several comparisons can still be performed. They show a satisfactory agreement between simulated and measured values. Nevertheless we can not catch, at this space resolution, the sudden sign inversion, which occurs at the monitor V2 (T=130).

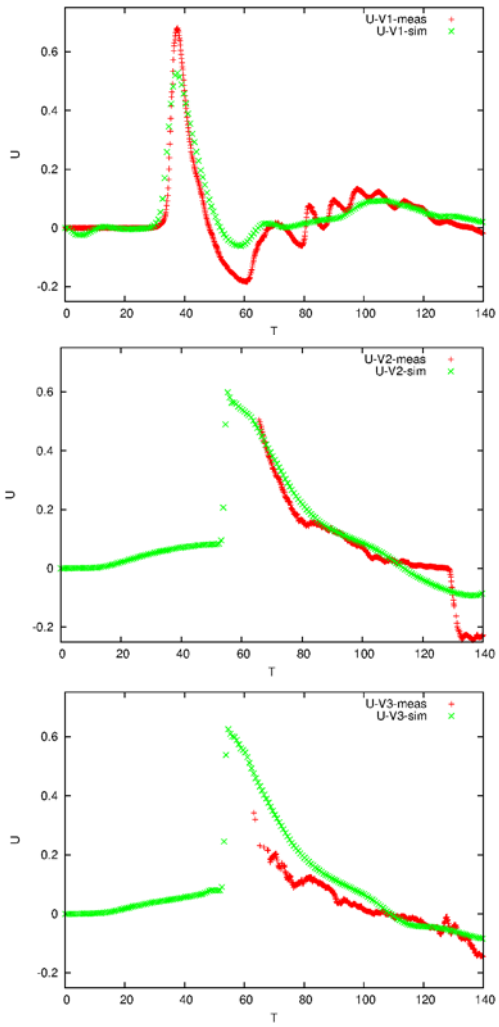

FIG. 6 TIME SERIES OF THE X-COMPONENT OF THE MEAN VELOCITY AT THE MONITORING POINTS V1-3. COMPARISONS BETWEEN THE SIMULATED AND MEASURED VALUES.

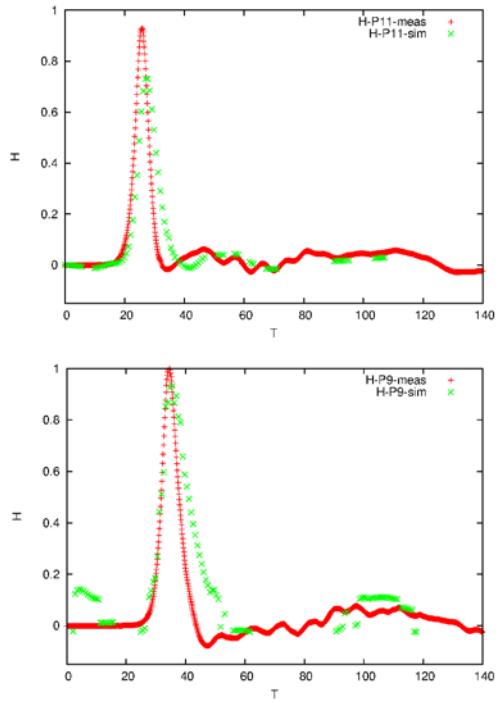

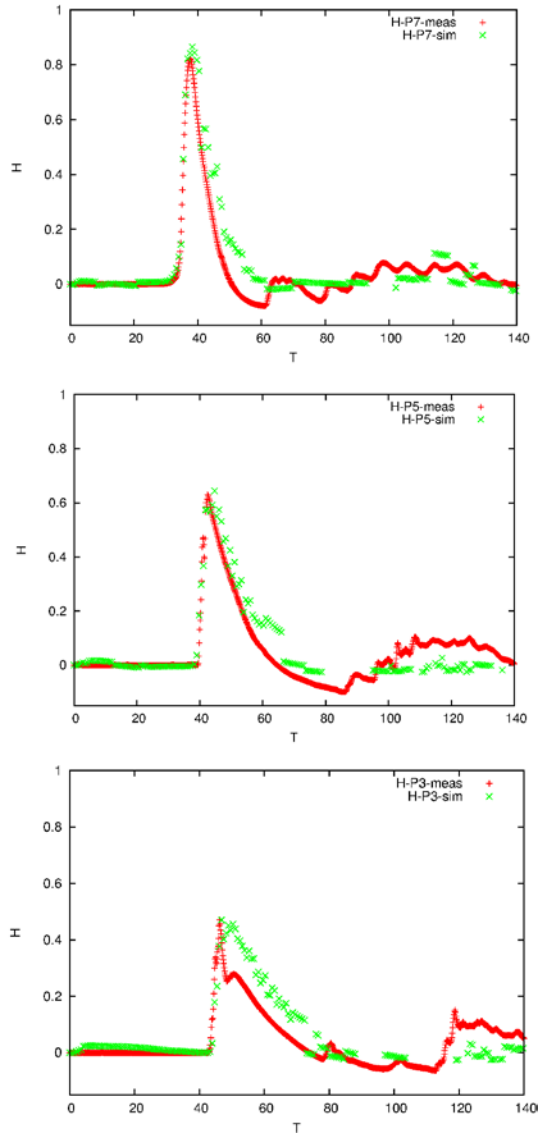

FIG. 7 SEA LEVEL TIME SERIES AT THE MONITORING POINTS P11, P9, P7, P5, P3. COMPARISONS BETWEEN THE SIMULATED AND MEASURED VALUES.

Two asymmetric rows of measuring probes (P1-12, FIG 1) are used to validate the estimation of the sea levels (FIG 7, FIG 8, FIG 9, FIG 10). All the curves clearly detect the passage of the solitary wave, which is followed by a secondary wave motion.

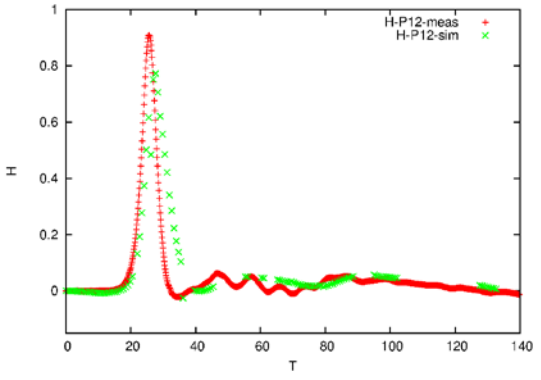

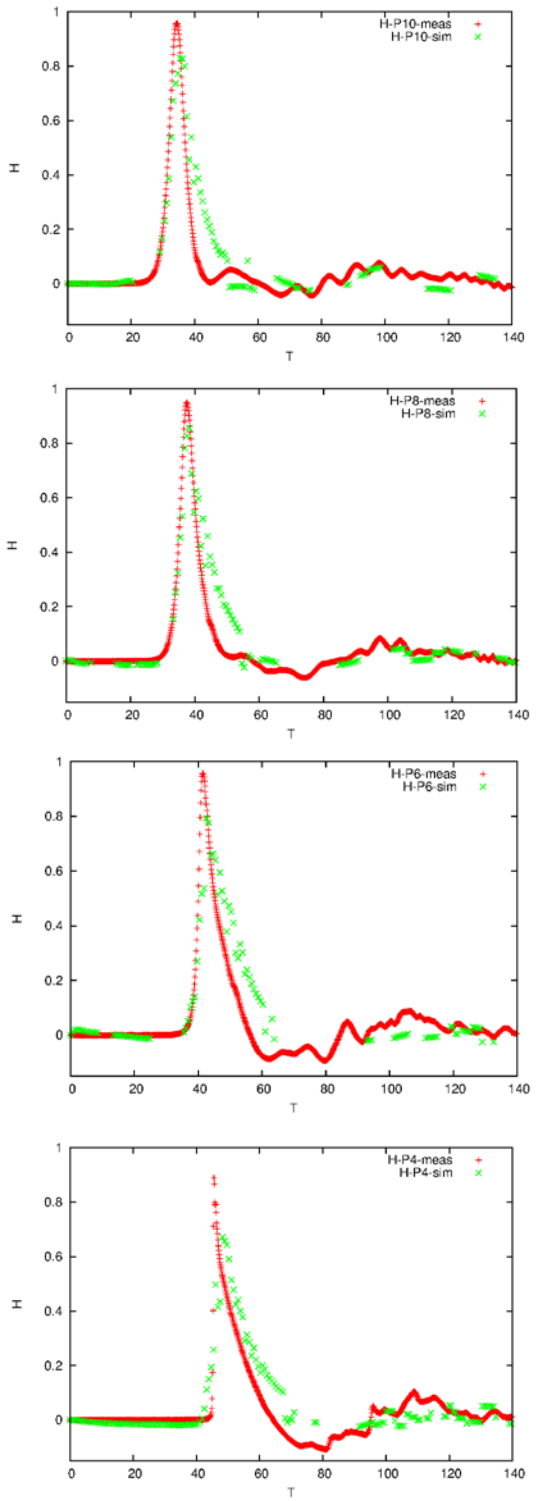

FIG. 8 SEA LEVEL TIME SERIES AT THE MONITORING POINTS P12, P10, P8, P6, P4. COMPARISONS BETWEEN THE SIMULATED AND MEASURED VALUES.

The increment in sea level is accompanied by an increase in the wave group velocity and the fundamental frequency. The normalized sea levels show its maximum around the promontory (refraction effects), as already stated (surface wave velocity goes with the square root of the fluid depth, under shallow

water approximations, so that power fluxes and sea level peaks tend to concentrate around promontories). The comparisons between all the simulated values and the corresponding measures show the good reliability of the model in estimating sea levels. Nevertheless we notice some lack of numerical data (a numerical probe invalidates some sea level values when the particle distribution around it is not considered enough populated) and some peak underestimations, occurring at this space resolution. We can also notice that we slightly overestimate the sea level after the peak, especially at probe P3. This could involve an underestimation of the fluid velocity in the breaking zone or an overestimation of the wave power. However, the first hypothesis seems being invalidated by the velocity comparisons (FIG 6) which do not show any underestimation in the breaking zone. Finally, we underline the importance of a correct evaluation of the velocity field down-flow the wave breaking to assess the tsunami destructive power and run up on land.

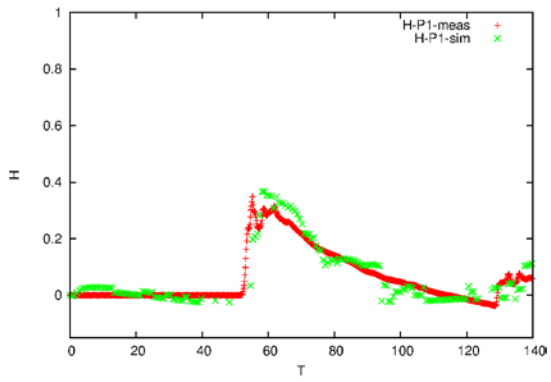

FIG. 9 SEA LEVEL TIME SERIES AT THE MONITORING POINT P1. COMPARISONS BETWEEN THE SIMULATED AND MEASURED VALUES.

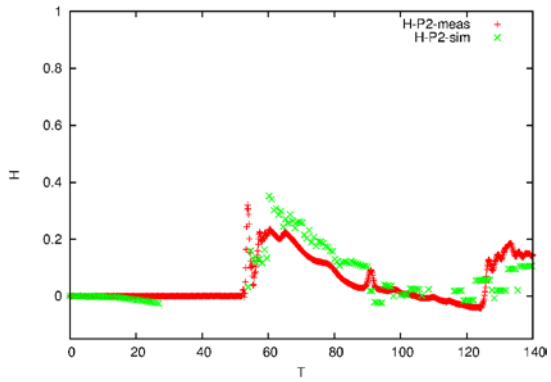

FIG. 10 SEA LEVEL TIME SERIES AT THE MONITORING POINT P2. COMPARISONS BETWEEN THE SIMULATED AND MEASURED VALUES.

Conclusions

A 3D SPH numerical model has been validated over a laboratory tsunami test case. The results show a good reliability of the model in representing the propagation of a solitary wave on a 3D shelf, both in terms of velocity and sea level.

The application field of this kind of validations can involve gravitational surface wave propagation in natural and artificial basins, the corresponding interactions with complex 3D shelves and structures, together with the associated coastal flood events.

ACKNOWLEDGMENTS

This work has been financed by the Research Fund for the Italian Electrical System under the Contract Agreement between RSE S.p.A. and the Ministry of Economic Development-General Directorate for Nuclear Energy, Renewable Energy and Energy Efficiency stipulated on July 29, 2009, in compliance with the Decree of November 11, 2012.

REFERENCES

Adami S., X. Y. Hu, N. A. Adams; "A generalized wall boundary condition for smoothed particle hydrodynamics"; Journal of Computational Physics, 231(2012): 7057–7075.

Agate G., R. Guandalini; "Strumenti numerici a scala di dettaglio per problemi idrodinamici in impianti idroelettrici"; Research Project Deliverable (ERSE protocol 08006002, February 2009).

Amicarelli A., G. Agate, R. Guandalini; "A 3D Fully Lagrangian Smoothed Particle Hydrodynamics model with both volume and surface discrete elements"; International Journal for Numerical Methods in Engineering 95(2013): 419–450, DOI: 10.1002/nme.4514

Amicarelli A., J-C. Marongiu, F. Leboeuf, J. Leduc, J. Caro; "SPH truncation error in estimating a 3D function"; Computers & Fluids 44(2011a): 279-296.

Amicarelli A., J.-C. Marongiu, F. Leboeuf, J. Leduc, M. Neuhauser, Le Fang, J. Caro; "SPH truncation error in estimating a 3D derivative"; International Journal for Numerical Methods in Engineering 87-7(2011b): 677-700.

Antuono M., A. Colagrossi, S. Marrone, C. Lugni; "Propagation of gravity waves through a SPH scheme with numerical diffusive terms"; Computer Physics Communications 182-4(2011): 866-877.

Basa M., N.J. Quinlan, M. Lastiwka; "Robustness and accuracy of SPH formulations for viscous flow"; International Journal for Numerical Methods in Fluids

60- 10(2009): 1127-1148.

Bauer A., V. Springel; "Subsonic turbulence in smoothed particle hydrodynamics and moving-mesh simulations"; Mon. Not. R. Astron. Soc. 423-3(2012): 2558–2578.

Delorme L., A. Colagrossi, A. Souto-Iglesias, R. Zamora-Rodriguez, E. Botia-Vera; "A set of canonical problems in sloshing, Part I: Pressure field in forced roll-comparison between experimental results and SPH"; Ocean Engineering 36(2009): 168–178.

Di Monaco A., Manenti S., Gallati M., Sibilla S., Agate G., Guandalini R.; "SPH modeling of solid boundaries through a semi-analytic approach"; Engineering Applications of Computational Fluid Mechanics 5/1 (2011): 1–15.

Farahani, R., Dalrymple, R., Hérault, A., and Bilotta, G. (2014). "Three-Dimensional SPH Modeling of a Bar/Rip Channel System." J. Waterway, Port, Coastal, Ocean Eng., 140(1), 82–99.

Ferrand M., D.R. Laurence, B.D. Rogers, D. Violeau, C. Kassiotis; "Unified semi-analytical wall boundary conditions for inviscid laminar or turbulent flows in the meshless SPH method"; International Journal for Numerical Methods in Fluids 71-4(2013): 446-472.

Grenier N., M. Antuono, A. Colagrossi, D. Le Touzé, B. Alessandrini; "An Hamiltonian interface SPH formulation for multi-fluid and free surface flows"; Journal of Computational Physics 228 (2009): 8380–8393.

Guandalini R., G. Agate; "Simulazione numerica di tecniche innovative per la rimozione controllata dell'interrimento dei serbatoi idroelettrici", Research Project Deliverable (RSE protocol 11000302, March 2011).

Hashemi M. R., R. Fatehi, M. T. Manzari; "A modified SPH method for simulating motion of rigid bodies in Newtonian fluid flows"; International Journal of Non-Linear Mechanics 47 (2012): 626–638.

ISEC -Inundation Science & Engineering Cooperative- http://isec.nacse.org

Kajtar J. B.; Monaghan J. J.; "On the swimming of fish like bodies near free and fixed boundaries"; European Journal of Mechanics B/Fluids 33(2012): 1–13.

Koukouvinis P.K., J.S. Anagnostopoulos, D.E. Papantonis; 2013; "An improved MUSCL treatment for the SPH-ALE method: comparison with the standard SPH method for the jet impingement case"; International Journal for Numerical Methods in Fluids, 71-9, 1152–1177. DOI: 10.1002/fld.3706

Kumar D., A.K. Patra, E.B. Pitman, H. Chi; "Parallel Godunov smoothed particle hydrodynamics (SPH) with improved treatment of Boundary Conditions and an application to granular flows"; Computer Physics Communications 184-10(2013): 2277-2286.

Le Veque R. J., D. L. George; "High-resolution finite volume methods for the shallow water equations with bathymetry and dry states, Advanced Numerical Models for simulating Tsunami Waves and Runup"; Advances in Coastal and Ocean Engineering (2007), H. Yeh, P. Lui, C. Synolakis eds.,World Scientific Publishing Co.

Macia F., L.M. Gonzalez, J.L. Cercos-Pita; A. Souto-Iglesias; "A Boundary Integral SPH Formulation - Consistency and Applications to ISPH and WCSPH"; Progress of Theoretical Physics 128-3(2012): 439-462.

Manenti S. "SPH modeling applied to sediment scouring"; Proc. 2nd Workshop Ports for Container Ships of Future Generations, TUHH University Hamburg (De), February 24-25 (2011).

Manenti S., G. Agate, A. Di Monaco, M. Gallati, A. Maffio, R. Guandalini, S. Sibilla; "SPH Modeling of Rapid Sediment Scour Induced by Water Flow"; 33rd IAHR Cong. 2009 August 9–14 Vancouver, British Columbia (Canada) 2009: 215-222.

Manenti S., A. Panizzo, P. Ruol, L. Martinelli; "SPH simulation of a floating body forced by regular waves"; 3rd Int. SPHeric Workshop, 4-6 June 2008, Lausanne (Switzerland), pp. 38-41.

Manenti S., S. Sibilla, M. Gallati, G. Agate, R. Guandalini; "SPH Simulation of Sediment Flushing Induced by a Rapid Water Flow"; Journal of Hydraulic Engeneering ASCE Volume 138-3(2012): 227-311.

Manenti S., S. Sibilla, M. Gallati, G. Agate, R. Guandalini; "SPH modeling of rapid multiphase flows and shock wave propagation"; Proc. Compdyn 2011 III ECCOMAS Corfu, Greece, 26–28 May (2011), ISBN: 978-960-99994-0-3.

Marongiu J.-C.; F. Leboeuf, J. Caro, E. Parkinson; "Free surface flows simulations in Pelton turbines using an hybrid SPH-ALE method"; J. Hydraul. Res. 47(2009): 40–49.

Maurel B., S. Potapov, J. Fabis, A. Combescure; "Full SPH

fluid–shell interaction for leakage simulation in explicit dynamics"; International Journal for Numerical Methods in Engineering 80-2(2009): 210–234.

Mayrhofer A., Rogers B.D., Violeau D., Ferrand M.; "Investigation of wall bounded flows using SPH and the uni fied semi-analytical wall boundary conditions"; Computer Physics Communications 184(2013): 2515–2527.

Monaghan J.J.; "Smoothed particle hydrodynamics"; Rep. Prog. Phys. 68(2005): 1703–1759.

Neuhauser M., J.-C. Marongiu, F. Leboeuf; "Coupling of the meshless SPH-ale method with a finite volume method"; Particle-based Methods III: Fundamentals and Applications – Proceedings of the 3rd International Conference on Particle based Methods, Fundamentals and Applications, Particles 2013: 939-948.

Omidvar P., P. K. Stansby, B. D. Rogers; "SPH for 3D floating bodies using variable mass particle distribution"; Int. J. Numer. Meth. Fluids 72-4(2013): 427-452.

Patel M.H., R. Vignjevic, J.C. Campbell; "An SPH Technique for Evaluating the Behaviour of Ships In Extreme Ocean Waves"; International Journal of Maritime Engineering 151(2009): 39-47.

Price, D.J.; "Smoothed Particle Hydrodynamics and Magnetohydrodynamics"; J. Comp. Phys. 231-3(2012): 759-794.

Price, D.J., J.J. Monaghan; "An energy conserving formalism for adaptive gravitational force softening in SPH and N-body codes"; MNRAS 374(2007), 1347-1358.

Souto-Iglesias A., L. Delorme, L. Pérez-Rojasa, S. Abril-Pérez; "Liquid moment amplitude assessment in sloshing type problems with smooth particle hydrodynamics"; Ocean Engineering 33(2006): 1462–1484.

Vacondio, R., B.D. Rogers, P. Stansby, P. Mignosa; "SPH Modeling of Shallow Flow with Open Boundaries for Practical Flood Simulation"; J. Hydraul. Eng. 138-6(2012):530–541.

Vila J.P.; "On particle weighted methods and Smooth Particle Hydrodynamics"; Mathematical Models and Methods in Applied Sciences 9.2(1999): 161-209.

Violeau D.; A. Leroy; 2014; "On the maximum time step in weakly compressible SPH"; Journal of Computational Physics, 256, 388-415.

Roberto Guandalini. He was born in Ferrara (Italy) on November 7, 1950 and graduated from Nuclear Engineering from Politecnico of Turin in 1975, where he joined the fast nuclear reactor research group until 1977. After that, he worked as researcher in many companies, mainly in the field of energy production, nuclear, thermal and hydro-electrical, as expert in advanced numerical simulation and as technical representative in many European Projects. Currently he is Leading Scientist in RSE SpA company in Milan, where he coordinates innovative research activities in the field of renewable energies, with special reference to the fluid dynamic modeling and the environmental impact aspects. He is also the company liaison officer for IAHR.

Giordano Agate. Researcher at Ricerca sul Sistema Energetico – RSE SpA. Research topics: Smoothed Particle Hydrodynamics (SPH, mesh-less Computational Fluid Dynamics for free-surface and multi-phase flows -e.g. floods, sloshing-), marine energy (numerical modeling). Software Manager of Sphera (SPH model for erosion and floods phenomena). Co-author of Hyper2D and Hyper3D (marine currents) and Tough2RdS (Carbon Capture and Storage, geothermal Energy Production and Compressed Air Energy Storage). 3 papers on International Peer-reviewed Journals, 15 papers on International Conferences. Contributions to more than 40 Research Projects.

Andrea Amicarelli. Researcher at Ricerca sul Sistema Energetico – RSE SpA (Research Institute, property of the Italian Ministry of Economic Development via GSE SpA; 2011-in progress). PhD in Hydraulic Engineering (2005-2008, Sapienza University of Rome, 2009). Research collaborator (ISPESL, 2007-2008, Italy). Post-Doc Research Engineer (LMFA Ecole Centrale de Lyon, C-Innov., 2009-2011, France). Maître de Conférences (Associate Professor) in "Mechanics, Mechanical Engineering and Civil Engineering" (Sec.60) and in "Meteorology, Physical Oceanography and Environmental Physics" (Sec.37): qualifications of the French Ministry of Research and Higher Education (2012). Editorial Board Member at "Studies in Engineering and Technology" and "Current Advances in Environmental Science". Research topics (fluid mechanics): Smoothed Particle Hydrodynamics (SPH, mesh-less Computational Fluid Dynamics for free-surface and multi-phase flows -e.g. floods, sloshing-); Lagrangian micromixing numerical models (for pollutant/scalar dispersion-e.g. air quality-). h-index=3 (Scopus) and 12 publications on international peer-reviewed journals (January 2014).

Sauro Manenti. Born in Arezzo (Italy) on January 1975, he received his PhD in Hydraulic Engineering on April 2008 from the University of Rome "Sapienza". Between 2008 – 2012 he was appointed adjunct professor at the University of Rome "Sapienza" in Coastal Engineering and Maritime Constructions. From December 2011 he is Assistant Professor at the University of Pavia (Italy) where he currently teaches Elements of Hydraulics at the UG level. Author and co-author of 37 publications on peer-revieved journals and conference proceedings. Major research interests: impulsve dynamics of multiphase flows with

rapidly varied interfaces; sediment scouring; dynamic analysis of offshore structures (breakwaters, wind turbine); wave mechanics (interactions in shallow water, risk analysis of waves damages, wave hindcasting); thermal-elastic analysis of massive composite structures; filtration in porous media.

Mario Gallati. Born in Montebello della Battaglia (Pavia, Italy) on February 1945. Full professor since 1984 at the University of Pavia (Italy) where he teaches Hydraulics at the UG level and Fluid Mechanics at PG level. Author and co-author of more than fifty publications on monographic books, peer-revieved journals and conference proceedings. Major research interests concern the experimental and numerical modelling of: Newtonian and non-Newtonian flows with moving boundaries and rapidly varied interfaces; fluid structure interaction; underwater explosion in saturated non-cohesive sediment; radio-frequency thermal ablation of liver cancer.

Stefano Sibilla. Born in Milan (Italy) in 1967, he graduated in Aeronautical Engineering in 1991 at Politecnico di Milano, where he also earned his PhD in Aerospace Engineering with a research on the Direct Numerical Simulation of turbulent flows. Since 2006 he has been associate professor in Hydraulics at the University of Pavia, where he currently teaches Hydraulic works at UG level and Numerical methods in fluid mechanics at PG level. He is member of the Steering Committee of the SPHERIC (Smoothed Paticle Hydrodynamics European Research Interest Community) group. He is author and co-author of 73 publications on peer-reviewed journals and conference proceedings. His major research interests include: numerical modelling of turbulent flows, Lagrangian methods in fluid mechanics, fluid-structure interaction problems, sediment scouring, diffusion phenomena in water bodies.